PHYSICAL REVIEW E **73**, 056310 (2006)

Effect of compaction history on the fluidization behavior of fine cohesive powders

Jose Manuel Valverde and Antonio Castellanos
Faculty of Physics, Universidad de Sevilla, Avenida Reina Mercedes s/n, 41012 Sevilla, Spain
(Received 10 February 2006; published 24 May 2006)

Fine particles agglomerate in the fluidized state due to the strength of interparticle attractive forces as compared to particle weight. Interparticle adhesion can be largely increased by consolidation stresses applied during powder handling. As a consequence, fragments of the consolidated powder may persist when the powder is fluidized, which gives rise to large agglomerates of strongly adhered particles in fluidization. This history-dependent effect can be minimized by coating the particles with surface additives such as silica nanoparticles. In this paper, we investigate the effect of high consolidation stresses σ_c previously applied to samples of silica-coated fine particles on their fluidization behavior. Our experimental measurements show that, even though homogeneous fluidization is still observed, the average agglomerate size and fractal dimension of the agglomerates increase as σ_c is increased. Bed expansion in the fluidized state is hindered by previously applied high consolidations, which we attribute to an increase of the largest stable size of mesoscopic fluid pockets. As a consequence, we observe that the initiation of macroscopic bubbling is delayed up to larger values of the fluid velocity.

DOI: 10.1103/PhysRevE.73.056310 PACS number(s): 47.55.Lm, 47.57.eb, 47.57.Gc

I. INTRODUCTION

The unpredictability of the collective behavior of fine particles represents a serious problem to many industrial applications. Fine powders exhibit poor flowability because of the prevalence of interparticle force on gravitational force, which hampers severely bulk processes such as delivery, dosage, mixing, and fluidization [1,2]. Powder behavior is influenced by many physical, chemical, and environmental variables. For example, experience shows that the flowability of a powder depends on how it was previously handled and processed. Interparticle adhesive forces increase due to powder compaction [3], which leads particles to aggregate in coherent large agglomerates. Thus strongly compressed samples of powder tend to flow worse after compaction, being usually difficult to be uniformly fluidized [4]. Coating fine particles with additives such as silica nanoparticles [3,5] minimizes the tendency of fine powders to cake when they are allowed to lie dormant for a long time between periods of use and/or they are subjected to very large compaction pressures. The main effect of coating the particles with these hard silica nanoparticles is to decrease the interparticle adhesion force for a given interparticle compressive force [2]. Adhesive contacts between coated fine particles are thus easily broken when fluidized by gas and, consequently, the fluidized bed exhibits smooth fluidization characterized by extremely high expansion and absence of visible gas bubbles [5,6]. In the fluidized regime, flowability is greatly enhanced, and high fluid-solid contact and reaction efficiency are promoted. A close look at the fluidized state reveals, however, that coated fine particles agglomerate in the fluidized regime due to the prevailing dominance of interparticle attractive force F_0 on particle weight W_p. Having a characterization tool of these agglomerates is desirable since particle agglomerates screen the external gas flow very effectively, thus having a relevant influence on the efficiency of gas-solid mixing. A theoretical analysis [4] on the dynamics of particle agglomeration in the uniformly fluidized bed shows that the ratio of agglomerate size d^* to particle size $d_p (k \equiv d^*/d_p)$ is given by the equation [4]

$$k \sim \mathrm{Bo}_g^{1/(D+2)}, \tag{1}$$

where $\mathrm{Bo}_g \equiv F_0/W_p$ is the granular Bond number, $D \equiv \ln N/\ln k$ is the fractal dimension of the agglomerates, which depends on the physical mechanism of particle agglomeration, and N is the average number of particles agglomerated. Typically, for micrometric sized particles coated with silica nanoparticles, Bo_g ranges in the interval from ~ 10 to ~ 1000 and $D \simeq 2.5$ [4], which gives a relative size of the agglomerates in the range $2 \sim < k < \sim 5$. In this paper, we investigate particle agglomeration in fluidized beds of silica-coated fine particles that had been previously subjected to high compaction pressures. Our goal is to find out the way in which previous powder compaction affects fluidization.

II. EXPERIMENTAL MATERIALS

We have tested cornstarch powder supplied to us by the New Jersey Center for Engineered Particulates. Field emission scanning electron microscope (FESEM) images [5] show that cornstarch particles are roundly shaped with a mean size of around $d_p = 15\ \mu$m. The density of cornstarch is $\rho_p \simeq 1550\ \mathrm{kg/m^3}$. Cornstarch particles are coated with 20 nm hydrophobic fumed silica nanoparticles by the magnetic assisted impaction coating (MAIC) method [5]. The weight percentage of additive is 1%, which gives 100% surface additive coverage (SAC) [5]. As seen in FSEM micrographs [5], silica nanoparticles are distributed in agglomerates of average size $d_{\mathrm{ag}} \sim 40$ nm. In this paper, we have also used xerographic toners, consisting of polymer particles with a mean size of $d_p \simeq 12.7\ \mu$m, particle density $\rho_p \simeq 1065\ \mathrm{kg/m^3}$, and coated with 7 nm fumed silica particles in concentrations of ~40%SAC and ~20%SAC. Additional description and measurements on the tensile strength and compressibility of these toner samples can be found in Ref. [3].

III. EXPERIMENTAL SETUP

Experiments were carried out using the Sevilla Powder Tester apparatus, which is based on the use of gas flow either to fluidize or compress the powder bed. The functioning of this device is described elsewhere in detail [2,7]. In this apparatus, the powder sample is held in a vertically oriented cylindrical vessel (4.42 cm internal diameter) resting on a sintered metal porous filter (5 μm pore size), which acts as a dry nitrogen distributor. By means of computer controlled valves and a mass flow controller, a controlled flow of dry nitrogen can be pumped upward or downward through the bed while the gas pressure drop across it is read from a differential pressure transducer. All the measurements are preceded by a convenient initialization of the sample into a reproducible state. This is accomplished by imposing a high upward directed gas flow that drives the powder into a bubbling regime. Once the bubbling bed has reached a stationary state, the gas flow is suddenly returned to zero. This conditioning process produces a repeatable starting condition for the powder sample as a preliminary to testing. The consolidation stress in this initial state at the bottom of the sample is given by its own weight per unit area W. To compress the powder beyond its own weight, the path of the gas is inverted and the downward directed gas flow is slowly increased. This process imposes a homogeneously distributed pressure on the powder. The consolidation stress at the bottom of the bed is thus increased up to $\sigma_c = W + \Delta p$, where Δp is the gas pressure drop across the powder. Once the sample is consolidated it is again subjected to a conditioning process prior to fluidization tests. The powder is then driven into the bubbling regime. Once the powder reaches a bubbling stationary state, the fluidizing gas velocity v_g is set down to a given value below the minimum bubbling velocity and the powder is allowed to reach a stationary and reproducible uniformly fluidized state. (According to the accuracy of our gas flow controller, the typical indeterminacy in the gas velocity is $\Delta v_g \simeq 0.01$ cm/s.) The bed height H is then measured by an ultrasonic emitter-receiver placed on top of the bed that determines distance accurately ($\Delta H \simeq 0.01$ cm) by sending an ultrasonic wave and measuring the time of reflection from the bed free surface. From the fluidized bed height and the particle density we compute the average particle volume fraction $\phi = m/(\rho_p SH)$, where m is the powder sample mass (typically 40 g) and S is the area of the gas distributor. The size of bed height fluctuations in the uniformly fluidized state is less than about ±0.1 cm, which results in a typical indeterminacy of $\Delta\phi \simeq 0.005$.

Particle agglomerates in the uniformly fluidized state are characterized by means of settling experiments, which consist of measuring the initial settling velocity v_s of the top free surface after the gas flow in the uniformly fluidized bed is suddenly stopped (the experimental procedure is described in detail in Ref. [8]). It has been shown that the relationship between v_s and ϕ can be well described by a modified Richardson-Zaki (RZ) equation, $v_s = v^*(1-\phi^*)^n$, that was obtained by considering agglomerates as effective spheres of size d^* [9]. Here $v^* = v_{p0}N/k$ is the settling velocity of an individual agglomerate, where $v_{p0} \simeq (1/18)\rho_p d_p^2 g/\mu$ is the settling velocity of a single particle (μ is the fluid viscosity and g the gravitational acceleration), $\phi^* = \phi k^3/N$ is the volume fraction filled by the agglomerates, and $n \simeq 5.6$ in the small-particle Reynolds number regime [9].

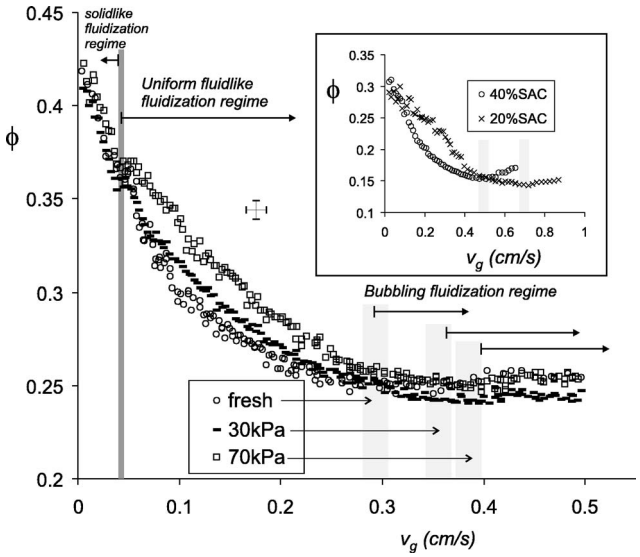

FIG. 1. Particle volume fraction ϕ of the fluidized bed vs superficial gas velocity v_g. Results are shown for powder samples previously subjected to different levels of consolidation stress (indicated). Inset: Particle volume fraction ϕ of the fluidized bed vs superficial gas velocity v_g for fresh samples of xerographic toners with different levels of surface additive coverage of the particles (indicated). The transitions to the solidlike regime and to the bubbling regime (as indicated by a saturation of bed expansion) are delineated. Typical error bars are also shown.

IV. RESULTS AND DISCUSSION

In Fig. 1, we have plotted data of the particle volume fraction ϕ as a function of the superficial gas velocity v_g in the fluidized bed. As seen for other fine powders [10], two regimes of fluidization are observable. For $v_g < 0.04$ cm/s ($\phi > \phi_J \simeq 0.35$), particles are jammed in a solidlike state. In this regime, part of the fluidized powder weight is held by permanent interparticle contacts while attractive forces between particles provide the weak solid structure with a small tensile strength [10]. At the jamming transition, particle agglomerates crowd in a volume fraction $\phi_J^* = \phi_J k^3/N$ which is close to the random loose packing of noncohesive spheres at the limit of zero gravity ($\phi_J^* \approx \phi_{\mathrm{RLP}} \simeq 0.56$ [11]) [12]. As the gas velocity is further decreased, these jammed agglomerates rearrange into a closer packed structure paralleling the jamming behavior of soft spheres [12]. In the close vicinity of the jamming transition, the particle volume fraction ϕ of the weak solid is thus determined by the particle volume fraction within the jammed agglomerates $\phi_{\mathrm{int}} = N/k^3 = k^{D-3}$. Figure 1 shows that in the solidlike regime there is not an appreciable difference in the ϕ versus v_g data among the samples previously consolidated at different stress levels. This result suggests that ϕ_{int} does not vary essentially with the previously applied stress. However, both the relative size of the agglomerates k and their fractal dimension D might differ as it

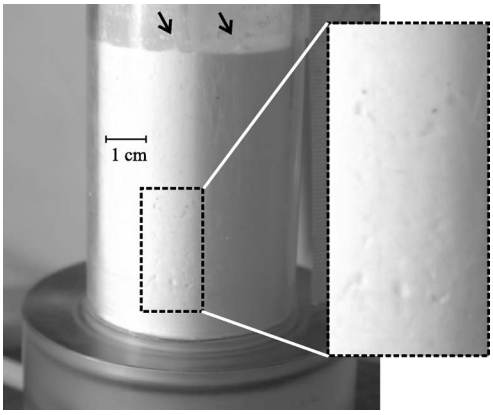

FIG. 2. Fluidized bed of cornstarch powder in the bubbling regime. Rising bubbles close to the wall can be seen in the zoom. Bubbles burst on the free surface can be also appreciated.

seems to indicate the clear divergence of the data (see Fig. 1) in the fluidlike regime $v_g > 0.04$ cm/s). We observe clearly that bed expansion in the fluidlike regime is hampered as the powder sample is previously consolidated to larger stresses. Furthermore, it can be seen in Fig. 1 that the onset of the bubbling regime, characterized by a minimum of ϕ due to the development of visible millimeter-sized gas bubbles (see Fig. 2), is delayed for the previously compacted samples. The delay of bubbling onset can be inferred more clearly from Fig. 3, where we plot the settling velocity v_s of the fluidized bed as a function of the superficial gas velocity v_g. Figure 3 shows that v_s and v_g are similar in the nonbubbling fluidization regime, indicating uniform fluidization which is characterized by homogeneous mixing of the gas and particles at the macroscopic level. As v_g is increased, we observe that v_s saturates at a gas velocity approximately coinciding with the gas velocity at which ϕ reaches a minimum. At this point, visible large gas bubbles are developed. Macroscopic bubbling is also recognized by strong oscillations of the bed height ($\Delta H \simeq 0.5$ cm) due to bubbles burst on the free surface. Figures 3 and 1 show that, even though it can be clearly appreciated that the onset of bubbling is delayed for the powder samples previously compacted to high consolidation stresses, the transition to the bubbling regime is not sharply defined. According to our measurements, the indeterminacy in the gas velocity at the onset of bubbling v_b is typically $\Delta v_g \simeq 0.03$ cm/s.

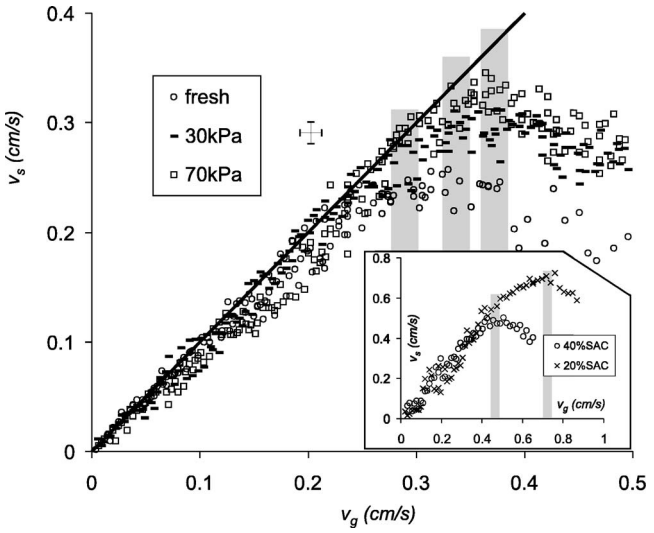

FIG. 3. Settling velocity v_s of the fluidized bed vs superficial gas velocity v_g. Results are shown for powder samples previously subjected to different levels of consolidation stress (indicated). The solid line represents the curve $v_s = v_g$. Inset: Settling velocity v_s of the fluidized bed vs superficial gas velocity v_g for fresh samples of xerographic toners with different levels of surface additive coverage of the particles (indicated). The vertical bars delineate the transition from uniform to bubbling fluidization as indicated by a saturation of settling velocity. Typical error bars are also shown.

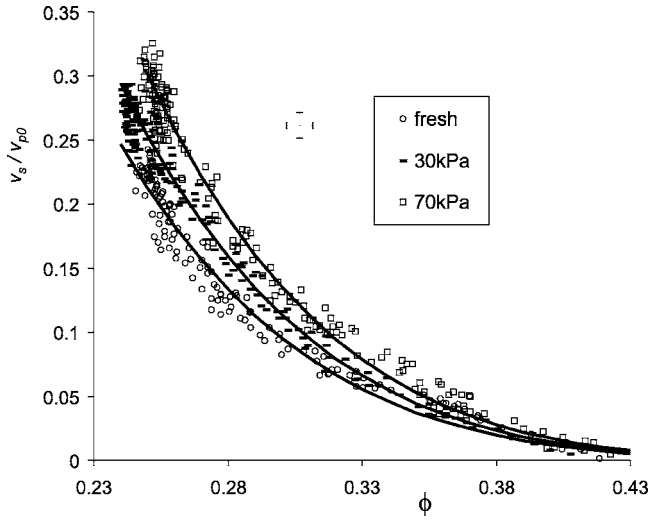

FIG. 4. Settling velocity of the fluidized bed (relative to single-particle settling velocity) v_s/v_{p0} vs the particle volume fraction ϕ for powder samples previously subjected to different levels of consolidation stress (indicated in the inset). Best fit curves of the modified RZ equation to the data are plotted. Typical error bars are also shown.

Since expansion of the fluidized bed in the fluidlike regime is directly related to the properties of particle agglomerates [9,13], our results indicate that previous compaction of the sample must have an effect, on the fluidized agglomerates. To further explore this effect, we have carried out settling tests of the uniformly fluidized bed that give us a measure of particle agglomerate properties [9]. In Fig. 4, we present data of the fluidized bed settling velocity v_s (relative to single-particle settling velocity v_{p0}) as a function of the particle volume fraction ϕ. Clearly, Fig. 4 indicates a nonnegligible effect of previous compaction on the properties of the fluidized agglomerates. As can be observed, the data corresponding to different levels of previous consolidation stress clearly differ. We see that, for a given value of ϕ, v_s increases as the previous consolidation stress applied is increased. The increase of v_s due to previous compaction is more noticeable for the region of small ϕ where long-ranged interactions are less relevant. We have also plotted in Fig. 4 the best fits of the modified RZ equation to the data. Results from these fits are $N=9.1$, $k=2.44$ (as-received fresh sample); $N=11.9$, $k=2.67$ (sample previously subjected to $\sigma_c \simeq 30$ kPa); and $N=15.4$, $k=2.91$ (sample previously sub-

jected to $\sigma_c \simeq 70$ kPa). According to the experimental scatter, the typical standard deviations are $\Delta N \simeq 1$ and $\Delta k \simeq 0.1$. Thus, the agglomerate size and number of particles agglomerated increase as σ_c is increased. On the other hand, we obtain that $\phi_{\text{int}} = N/k^3 \simeq 0.625$ is approximately the same for the three samples as it was anticipated from our previous analysis of the results in the solidlike regime. From the value of $\phi_J \simeq 0.35$ at the jamming transition and the values of N and k derived, it is obtained that agglomerates of the different samples jam at approximately the same volume fraction $\phi_J^* = \phi_J k^3/N \simeq 0.56$, which matches the random loose packing fraction of noncohesive spheres at the limit of zero gravity [11]. For the fractal dimension of the agglomerates, we obtain $D = \ln N/\ln k \simeq 2.47$ (as-received fresh sample), $D \simeq 2.52$ (sample previously subjected to $\sigma_c \simeq 30$ kPa), and $D \simeq 2.56$ (sample previously subjected to $\sigma_c \simeq 70$ kPa). Note that, as seen for other fine powders [9], these values are close to $D = 2.5$ in agreement with a diffusion-limited particle-to-cluster aggregation model (DLA) [14]. (As discussed in previous works [15], D is a robust parameter of the fit by the modified RZ equation.) In the DLA model, the number of contacts per particle within the agglomerate is around two since cohesive particles cannot penetrate inside the agglomerate to stick at more than one point of contact. The increase of D as σ_c is increased is thus attributable to the existence within the agglomerates of particles contacting with more than two particles. These contacts must correspond to strongly adhesive interparticle joints previously formed in the highly compacted state that cannot be broken by fluidization thus persisting in the fluidlike regime. We would have therefore compact fragments in the fluidized state intervening in the dynamic agglomeration process that contribute to increase the equilibrium size and fractal dimension of the agglomerates formed in the fluidized state.

As can be seen in the insets of Figs. 1 and 3, the effect of high compaction on the fluidization behavior is analogous to the effect of decreasing the surface additive coverage (SAC) of silica. Small SAC allows for strongly adhesive contacts between bare polymer surfaces of the toner particles [2] in the solid state. Thus, even for fresh samples previously subjected to small consolidations, small SAC leads to the persistence of solidlike fragments in fluidization that contribute to increase the size of the agglomerates formed in the fluidized bed. It is thus predictable that the effect of compaction history should be more relevant for uncoated fine powders, which usually exhibit heterogeneous fluidization. Remarkably, a similar phenomenon has been observed in fragmentation of colloidal suspensions of strongly cohesive particles [16].

According to the scaling law given by Eq. (1), the average agglomerate sizes obtained would correspond to average granular Bond number and attractive force $\text{Bo}_g \simeq 50 \rightarrow F_0 \simeq 1.5$ nN (as received fresh sample), $\text{Bo}_g \simeq 90 \rightarrow F_0 \simeq 2.3$ nN (sample previously subjected to $\sigma_c \simeq 30$ kPa), and $\text{Bo}_g \simeq 130 \rightarrow F_0 \simeq 3.5$ nN (sample previously subjected to $\sigma_c \simeq 70$ kPa). The attractive force between the dry and uncharged fluidized particles F_0 arises mainly from the van der Waals interaction $F_0 \simeq A d_a/(24 z_0^2)$, where $z_0 \simeq 4$ Å is the distance of closest approach between two molecules, A is the Hamaker constant, and d_a is the typical size of the surface asperities [2]. For our powder particles coated with 100%SAC, interparticle contacts will occur between silica agglomerates of size $d_a \simeq 40$ nm, which can be used as the typical size of surface asperities, whereas for silica $A \simeq 1.5 \times 10^{-19}$ J [17]. Using these values we estimate $F_0 \simeq 1.6$ nN, in quite good agreement with our previous estimation. In most powders it is difficult to obtain exact values of the surface asperity since it requires a tedious profilometry analysis of the surface roughness by AFM. Moreover, d_a usually shows a wide distribution [2]. Settling experiments and Eq. (1) can be an alternative tool to estimate the interparticle attractive force.

Let us return to the question on the effect of previous compaction on the expansion of the fluidized bed. If the collective interaction between bubbles is neglected, we may obtain a rough estimation of the maximum size of gas pockets in the uniformly fluidized bed by using the criterion proposed by Harrison *et al.* [18]. From experimental observations on fluidized beds, Harrison *et al.* derived that isolated gas pockets of size D_b are split when their rising velocity $U_b \simeq 0.7\sqrt{gD_b}$ [19,20] exceeds the settling velocity of a single particle v_{p0}. For our fluidized bed model of agglomerates we must modify the criterion to use the settling velocity of an agglomerate $v^* = v_{p0} N/k$ instead of that of a single particle. The Harrison *et al.* criterion modified for agglomerate fluidization is thus $0.7\sqrt{gD_b} \sim v_{p0} N/k$. Using the values of N and k derived from the settling experiments we calculate $D_b \simeq 320\ \mu\text{m} \simeq 8.9 d^*$ (as received fresh sample), $D_b \simeq 460\ \mu\text{m} \simeq 11.6 d^*$ (sample previously subjected to $\sigma_c \simeq 30$ kPa), and $D_b \simeq 650\ \mu\text{m} \simeq 15 d^*$ (sample previously subjected to $\sigma_c \simeq 70$ kPa). The values of D_b/d^* are around 10, which is the order of magnitude of the limiting value obtained by Harrison *et al.* that distinguished bubbling from uniform fluidization behavior. Accordingly, we observe both regimes in our fluidized beds. Moreover, these estimations explain the effect of previous compaction on bed expansion when the system transits to the fluidlike regime (Fig. 1). The larger value of the maximum stable size of gas pockets results in less uniform fluidization at the mesoscopic level and, consequently, must hinder bed expansion. At low gas velocities the size of these individual gas pockets, is however, insufficient for them to reach a macroscopic stable size that might give rise to bubbling. The collective interaction between gas pockets at high gas velocities through splitting-coalescence mechanism ultimately leads to the development of macroscopic gas bubbles of size larger than Harrison's maximum stable size [21] (onset of bubbling). According to our results, the volume fraction of agglomerates at incipient bubbling is almost independent of previous compaction, $\phi_b^* \simeq 0.4$, which implies that the number of agglomerates per unit volume is smaller for the larger agglomerates of the previously compacted samples. Equivalently, it can be said that macroscopic bubbles develop for the same value of the volume fraction of gas pockets, $1 - \phi_b^* \simeq 0.6$, which is given by the number of gas pockets per unit volume n_b times their average volume. Since gas pockets are larger for the previously compacted samples, the development of bubbles occurs for smaller values of n_b for these samples, as might be reasonably expected. According to Geldart's experimental observations [22], bubble sizes between one and two orders

of magnitude larger than Harrison's maximum stable size can be developed in bubbling beds, which according to our previous estimations would give millimeter sized bubbles in our system, in agreement with our experimental observations (see Fig. 2).

V. CONCLUSION

In conclusion, it has been shown that the history of fine powders may play an important role in their fluidization behavior. Our work shows that the uniformity of fluidization at the mesoscopic level is hampered by previous compaction. We have seen that compaction of the powder sample to high stresses produces larger agglomerates in the fluidized state due to the previous formation of strongly adhesive contacts in the compacted solid that cannot be broken by fluidization. As the previously applied consolidation stress is increased, the average size of agglomerates increases and the expansion of the fluidized bed is hindered due to the larger maximum stable size of local gas pockets. Furthermore, the onset of macroscopic bubbling is delayed up to higher values of the gas velocity. We believe that our experimental procedure could be useful for evaluating the effectiveness of powder conditioning methods such as vibration, sound pulses, or magnetic excitation. These processes are used in industry in order to break large agglomerates, thus assisting fluidization of cohesive powders.

ACKNOWLEDGMENTS

This research has been supported by the Spanish Government Agency Ministerio de Ciencia y Tecnologia (Contract No. BFM2003-01739) and Junta de Andalucia (Contract NO. FQM 421). We acknowledge also the New Jersey Center for Engineered Particulates for supplying us with the cornstarch powder sample.

[1] J. P. K. Seville *et al.*, *Processing of Particulate Solids* (Chapman and Hall, London, 1997).
[2] A. Castellanos, Adv. Phys. **54**, 263 (2005).
[3] J. M. Valverde *et al.*, Powder Technol. **97**, 237 (1998).
[4] A. Castellanos, J. M. Valverde, and M. A. S. Quintanilla, Phys. Rev. Lett. **94**, 075501 (2005).
[5] J. Yang *et al.*, Powder Technol. **158**, 21 (2005).
[6] J. M. Valverde, A. Castellanos, P. Mills, and M. A. S. Quintanilla, Phys. Rev. E **67**, 051305 (2003).
[7] J. M. Valverde *et al.*, Rev. Sci. Instrum. **71**, 2791 (2000).
[8] J. M. Valverde *et al.*, Europhys. Lett. **54**, 329 (2001).
[9] A. Castellanos, J. M. Valverde, and M. A. S. Quintanilla, Phys. Rev. E **64**, 041304 (2001).
[10] J. M. Valverde, A. Castellanos, and M. A. S. Quintanilla, Phys. Rev. Lett. **86**, 3020 (2001).
[11] G. Y. Onoda and E. G. Liniger, Phys. Rev. Lett. **64**, 2727 (1990).
[12] J. M. Valverde, M. A. S. Quintanilla, and A. Castellanos, Phys. Rev. Lett. **92**, 258303 (2004).
[13] C. H. Nam *et al.*, AIChE J. **50**, 1776 (2004).
[14] T. A. Witten and L. M. Sander, Phys. Rev. Lett. **47**, 1400 (1981).
[15] J. M. Valverde and A. Castellanos, AIChE J. **52**, 838 (2006).
[16] Y. Tatek *et al.*, Powder Technol. **143-144**, 117 (2004).
[17] S. Ross and I. D. Morrison, *Colloidal Systems and Interfaces* (Wiley-Interscience, New York, 1988).
[18] D. Harrison *et al.*, Trans. Inst. Chem. Eng. **39**, 202 (1961).
[19] J. F. Davidson *et al.*, Annu. Rev. Fluid Mech. **9**, 55 (1977).
[20] A. C. Hoffmann and J. G. Yates, Chem. Eng. Commun. **41**, 133 (1986).
[21] M. Horio and A. Nonaka, AIChE J. **33**, 1865 (1987).
[22] M. J. Rhodes, *Introduction to Particle Technology* (Wiley, Chichester, 1998).